

K. KOWALSKI^{*,‡}, M. JURCZYK^{*}

POROUS MAGNESIUM BASED BIONANOCOMPOSITES FOR MEDICAL APPLICATION

POROWATE BIONANOKOMPOZYTY NA BAZIE MAGNEZU DO ZASTOSOWAŃ MEDYCZNYCH

In this study, Mg-10 wt.% hydroxyapatite nanocomposites and their scaffolds were synthesized using a combination of mechanical alloying and a powder metallurgy methods. The phase and microstructure analysis was carried out using X-ray diffraction, scanning electron microscopy, and the properties were measured using hardness and corrosion testing apparatus. According to the Scherrer method for XRD profiles, the average size of mechanically alloyed Mg+10 wt. % HA for 20 h powders was of order of 21 nm for Mg. The Vickers hardness of the Mg-10 wt.% HA reached 87 HV_{0.3}. The corrosion resistance of the bulk Mg-10 wt.% HA nanocomposite and its scaffolds was investigated in the Ringer's solution. The potentiodynamic corrosion resistance tests revealed that the porosity of the Mg-10 wt.% HA nanocomposite scaffolds had no negative effects compared to microcrystalline Mg.

Keywords: Magnesium, Hydroxyapatite, Biocomposites, Mechanical alloying

1. Introduction

Mg and Mg-based alloys are preferred materials in the production of implants in medical applications [1]. Comparing to other biomedical materials they possess several advantages. The fracture toughness of magnesium is greater than ceramic and polymer biomaterials, while the elastic modulus and compressive yield strength of magnesium are closer to those of natural bone [2]. Mechanical properties of Mg-based biomaterials should prevent of stress-shielding effect occurring. Another advantage of magnesium is its excellent biocompatibility. Magnesium is essential to human metabolism and is naturally found in bone tissue [1]. However, poor corrosion resistance in the body fluids environment is the main limitation of use magnesium based biomaterials. Low corrosion resistance results in the rapid and inhomogeneous degradation of implants which can cause a reduction in the mechanical integrity of the implant before the repaired tissue is sufficiently healed [3]. These biomaterials have also relatively poor tribological properties because of their low hardness.

During last years, interest in the study of nanostructured materials has been increasing. These materials exhibit many interesting and unexpected properties with a number of potential medical applications [4, 5]. The present study examines the structure, microhardness and corrosion resistance of bulk Mg-10 wt.% HA bionanocomposite and its scaffold.

2. Experimental

Mechanical alloying (MA) was performed under an argon atmosphere using a SPEX 8000 Mixer Mill. The start-

ing materials included magnesium (325 mesh, 99.8%) and hydroxyapatite (99.9%). The vial was loaded and unloaded in a Labmaster 130 glove box under a high-purity argon atmosphere. The mixed powders were mechanically alloyed for 20h. The blended Mg-10 wt.% HA was mixed with ammonium hydrogen carbonate (NH₄HCO₃), which was used as the space-holder material. The size of the space-holder particles was 500-800 μ m.

The mixture containing MA Mg-10 wt.% HA powder and NH₄HCO₃ was uniaxially pressed at a compacting pressure of 400 MPa. The green compacts were sintered under a vacuum of 10⁻⁴ Torr in two steps. The first step was conducted at 180°C for 2 h to remove the space-holder particles. In the second step, the compacts were heat treated at 450°C for 24 h. Porous Mg-10 wt.% HA composites with porosity of 45% were fabricated by adding 30 wt.% ammonium hydrogen carbonate to the powder mixture. For all tests, the discs of bulk Mg-10 wt.% HA composites, Mg-10 wt. % HA scaffolds and microcrystalline Mg were used.

The microstructure of the samples during different processing stages was investigated using a Panalytical Empyrean XRD with CuK α_1 radiation. Scanning electron microscopy (SEM) with energy dispersive spectrometer (EDS) were used to characterize the synthesized materials. The Vickers microhardness of the bulk samples was measured using a microhardness tester by applying a load of 300 g on the polished surfaces of the samples. The Solartron 1285 potentiostat was applied for corrosion measurements. The corrosion potentials (E_C) and corrosion current densities (I_C) were estimated from the Tafel extrapolations of the corrosion curves, using Cor-

^{*} INSTITUTE OF MATERIALS SCIENCE AND ENGINEERING, POZNAN UNIVERSITY OF TECHNOLOGY, POZNAN, POLAND

[‡] Corresponding author: kamil.h.kowalski@doctorate.put.poznan.pl

rView software. Using the 3D optical profiler, Veeco WykoR® NT 1100, the standard roughness parameters were estimated.

3. Results and discussion

The magnesium-10 wt.% HA scaffold nanocomposite was prepared. X-ray diffraction was employed to examine the effects of mechanical alloying on the Mg-10 wt.% HA. Figs. 1a, b present the XRD patterns of the initial Mg (ICDD: 00-035-0821) and HA (ICDD: 01-075-9526) powders. During the MA process, the intensity of the Mg Bragg reflections decrease with increasing milling time. The microstructure that forms during MA consists of layers of the starting material. The lamellar structure is increasingly refined during further mechanical alloying. After 20 h of mechanical alloying the sample shows cleavage fracture morphology and inhomogeneous size distribution. According to the Scherrer method for XRD profiles, the average size of mechanically alloyed Mg+10 wt. % HA for 20 h powders was of order of 21 nm for Mg. The formation of the bulk nanocomposites was achieved by annealing the MA powders in a high purity argon atmosphere (99.99%) at 450°C for 24 h. The XRD analysis of the Mg-10 wt.% HA scaffold with a porosity of 45% revealed the presence of hexagonal type structure ($a = 3.209 \text{ \AA}$ and $c = 4.898 \text{ \AA}$) and trace of MgO phase.

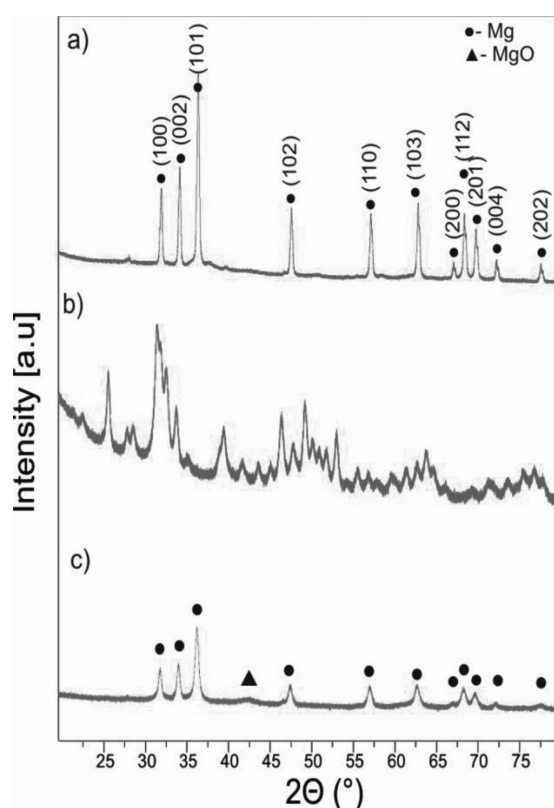


Fig. 1. XRD patterns of: a) initial Mg powder, b) initial HA powder, c) Mg-10 wt.% HA biocomposite after the 20 h MA process

The high deformation during the MA leads to the large dislocation density and formation of the nanometer size subgrains. Nanograined materials with a very high number of atoms on the surface have large surface energy. Thus they

exhibit entirely different behavior compared to micron sized grains.

The results of EDS analysis of the surface of sintered Mg-10 wt.% HA composite is shown in Fig. 2. It can be confirmed that synthesized scaffold mainly consists of Mg matrix with elements of Ca, P and O. The Ca/P ratio is 1.79, which is corresponding to hydroxyapatite.

The Vickers hardnesses for the Mg-10 wt.% HA nanocomposite reached 87 HV_{0.3} and is two times greater than that of pure microcrystalline Mg (51 HV_{0.3}). This effect is directly associated with structure refinement and obtaining a nanostructure.

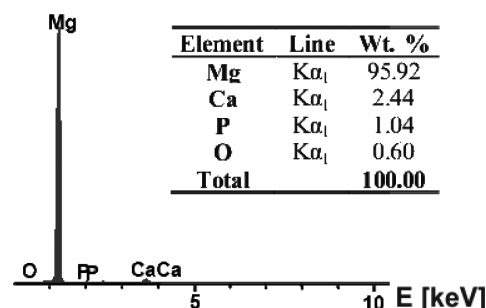


Fig. 2. EDS surface spectrum of the bulk Mg-10 wt.% HA sample

An optical micrograph of the Mg-10 wt.% HA nanocomposite scaffold with 45% porosity is shown in Fig. 3a. This scaffold exhibited wide cavities, which were 30-350 μm in diameter. The smooth Mg-10 wt.% HA surface is presented in Fig. 3b. The relative density of the bulk Mg-10 wt.% HA nanocomposite was measured to be 99.1 %. The Young's modulus of the studied Mg-HA nanocomposites can be significantly reduced by the introduction of porosity. Generally, large variations in the elastic modulus and plateau stress of the scaffolds can be a consequence of chemical compositions, pore morphologies, pore sizes, pore size distributions, shape and thickness of struts and the different compressive strength test parameters employed (sample geometry, size, and loading speed).

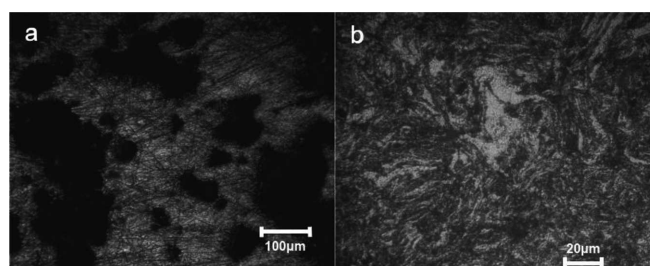


Fig. 3. OM micrograph of Mg-10 wt.% HA scaffold (a) and bulk Mg-10 wt.% HA sample

Potentiodynamic polarization curves of pure magnesium and bulk Mg-10 wt.% HA nanocomposite are shown in Fig. 4. The polarization data of sintered materials including corrosion potentials (E_c) and corrosion current densities (I_c) are presented in Table 1. The results obtained for nanocrystalline Mg-10 wt.% HA are close to the microcrystalline magnesium. Addition of HA shifts corrosion potential to the less negative value.

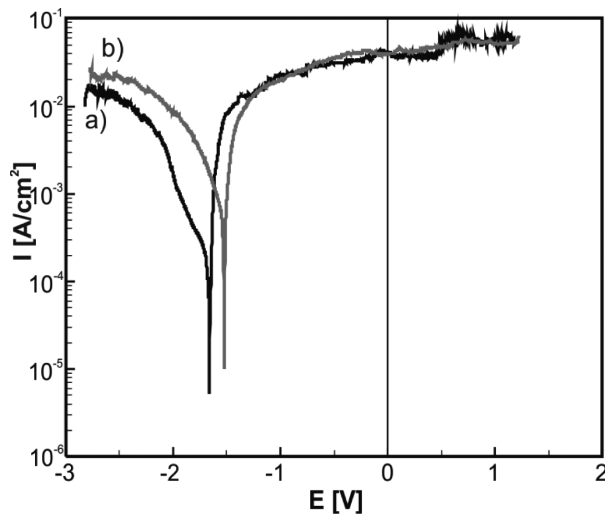


Fig. 4. Potentiodynamic polarization curves of: microcrystalline magnesium (a) and Mg -10 wt.% HA composite scaffold (b) in Ringer's solution at 23°C

TABLE 1

Vickers hardness, corrosion current densities and corrosion potentials of studied Mg-10 wt.% HA nanocomposites compared to microcrystalline magnesium

Material	HV _{0.3}	Corrosion properties	
		I _c [A/cm ²]	E _c [V]
microcrystalline Mg	51	2.3·10 ⁻⁴	-1.660
nanocomposite Mg-10 wt.% HA	87	8.25·10 ⁻⁴	-1.561

Roughness on polished bulk Mg-10 wt.% HA nanocomposite and Mg-10 wt.% HA scaffold with 45% porosity are also investigated. The pores in the polished surface result in the formation of valleys and peaks. It has been proven that surface properties of medical implants determine successful osseointegration. The scaffold with a 45% porosity had an average surface roughness in the range of 80-400 μm. Webster and Ejiofor have reported, that the optimal pore size for the cell attachment, differentiation and ingrowth of osteoblasts and

vascularization to be approximately 200-500 μm [6]. Large pores formation, supporting cell growth and proliferation, occurs during space-holder sintering process. The results published recently by Sul et al. showed that morphology of different commercially available clinical implants differed due to the surface modification techniques used during manufacture [7].

4. Conclusions

A new kind of biomedical Mg-10 wt.% HA scaffold was synthesized by mechanical alloying and powder metallurgy process. The Mg-10wt. HA nanocomposite exhibit a two time higher microhardness compared to microcrystalline magnesium. The scaffold with a 45% porosity had an average surface roughness values in the range of 80-400 μm. The Mg -HA composite has a lower corrosion resistance measured in Ringer solution compared to pure magnesium. The main advantage of the study is to establish that the Mg-10 wt.% HA composite scaffolds can become an innovative material resource serving for a new generation of biomaterials.

Acknowledgements

The work was financed by National Science Centre Poland under the decision no. DEC-2013/11/B/ST8/04394.

REFERENCES

- [1] N. Li, Y. Zheng, J. Mater. Sci. Technol. **29**, 489- 02 (2013).
- [2] M.P. Staiger, A.M. Pietak, J. Huadmai, G. Dias, Biomaterials **27**, 1728-34 (2006).
- [3] H.S. Brar, M.O. Platt, M. Sarntinoranont, P.I. Martin, M.V. Manuel, JOM **61**, 31-4 (2009).
- [4] B.C. Ward, T.J. Webster, Mater. Sci. Eng. C **27**, 575-8 (2007).
- [5] K. Niespodziana, K. Jurczyk, J. Jakubowicz, M. Jurczyk, Mater. Chem. Phys. **123**, 160-5 (2010).
- [6] T.B. Webster, J.U. Ejiofor, Biomaterials **25**, 4731-9 (2004).
- [7] Y.T. Sul, B.S. Kang, C. Johansson, H.S. Um, C.J. Park, T. Al-bektsson, J. Biomed. Mater. Res. A **89**, 942-50 (2009).

Received: 20 November 2014.